Journal of Alloys and Compounds 754 (2018) 283–296

Contents lists available at ScienceDirect

Journal of Alloys and Compounds

journal homepage: http://www.elsevier.com/locate/jalcom

Optimum parameters and kinetic analysis for hot working of a solution-treated Mg-Zn-Y-Mn magnesium alloy

Jianqiang Hao [a, b], Jinshan Zhang [a, b, *], Chunxiang Xu [a, b], Kaibo Nie [a, b]

[a] College of Materials Science and Engineering, Taiyuan University of Technology, Taiyuan, 030024, China
[b] Shanxi Key Laboratory of Advanced Magnesium-based Materials, Taiyuan, 030024, China

ARTICLE INFO

Article history:
Received 21 December 2017
Received in revised form
25 April 2018
Accepted 26 April 2018
Available online 30 April 2018

Keywords:
Magnesium alloy
Constitutive equation
Kinetic model
Processing map

ABSTRACT

The flow behavior, dynamic recrystallization (DRX) evolution and hot workability of the solution-treated $Mg_{94}Zn_{2.5}Y_{2.5}Mn_1$ (at%) alloy were investigated by hot compression tests. Compression tests were performed in the temperature range of 350–500 °C and the strain rate range of 0.001–1 s^{-1} on a Gleeble-1500D thermo-mechanical simulator. Using regression analysis for the constitutive equation of the flow behavior, the average activation energy of deformation and the stress exponent were determined to be 302.22 kJ/mol and 8.60452, respectively. The flow stress of the $Mg_{94}Zn_{2.5}Y_{2.5}Mn_1$ alloy predicted by the proposed models well agrees with experimental results. The kinetic model of DRX was proposed based on the analysis of true stress-strain data, which can be described as $X_{DRX} = 1 - \exp[-2.15((\varepsilon - \varepsilon_c)/\varepsilon^*)^{1.51}]$. The DRX kinetic model was validated by means of microstructure observation. Furthermore, processing maps were developed and analyzed based on the dynamic material model (DMM). The flow instability regions and stability regions were identified based on the processing maps; the optimum domain for hot working of the experimental alloy are temperatures ranging from 400 °C to 450 °C and strain rates ranging from 0.001 s^{-1} to 0.01 s^{-1}. Finally, a hot extrusion test was performed according to the optimum deformation parameters. The deformed sample exhibited a good surface quality and excellent mechanical properties, which verified the reasonability of the optimal deformation parameters.

1. Introduction

Magnesium alloys, being the lightest metallic structural materials, are used in automation, transportation and electronics because of high specific strength, specific stiffness and good recyclability [1–7]. In recent years, Mg-Zn-Y series alloys have attracted increasing attention due to their unique microstructures and excellent mechanical properties [8–16]. Depending on the Y/Zn atomic ratio, three kinds of ternary equilibrium phases can be formed in Mg-Zn-Y alloys. They are X-phase ($Mg_{12}ZnY$, long-period stacking ordered (LPSO) structure), W-phase ($Mg_3Zn_3Y_2$, cubic structure) and I-phase (Mg_3Zn_6Y, icosahedral quasi-crystal structure). Among these phases, the X-phase (LPSO phase) is considered as a good strengthening phase because of its unique crystal structure, high strength, high hardness and excellent thermal stability [6,8,9,12,14–16]. $Mg_{97}Y_2Zn_1$ (at%) alloy processed by rapidly solidified power metallurgy (RS P/M) was reported to exhibited a high yield strength of 610 MPa and a relatively high tensile ductility of 5% at room temperature [12,17]. The excellent mechanical properties result from the fine grain size and the formation of a novel 18R LPSO phase [14,15]. Although the Mg-Zn-Y alloy containing the LPSO phase has excellent mechanical properties, its commercial application is restricted largely by the high cost of RS P/M processing method. Moreover, the mechanical properties of the Mg-Zn-Y alloy decrease severely when using conventional casting technology [12]. To improve the mechanical properties of Mg-Zn-Y alloys containing the LPSO phase, a modification in composition is necessary by adding other alloying elements. Mn is an important alloying element for magnesium alloys. Adding Mn to magnesium alloys can refine grains sizes and improve the corrosion resistance and mechanical properties [12,18,19]. In addition, Li et al. [20] investigated the effects of Mn on the microstructure and mechanical properties of the $Mg_{95}Zn_{2.5}Y_{2.5}$ (at%) alloy with a low content Y/Zn ratio (at%). The results showed that the addition of Mn could promote the formation of X-phase while hindering the formation of

* Corresponding author. College of Materials Science and Engineering, Taiyuan University of Technology, Taiyuan, 030024, China.
E-mail address: jinshansx@tom.com (J. Zhang).

https://doi.org/10.1016/j.jallcom.2018.04.292
0925-8388/

W-phase and that the $Mg_{95}Zn_{2.5}Y_{2.5}Mn_1$(at%) alloy exhibited the best mechanical properties. Yang et al. [21] studied the spheroidizing behavior of W-phase during solid-solution treatment in the $Mg_{95}Zn_{2.5}Y_{2.5}Mn_1$(at%) alloy and found that the W-phase can transform from a continuous network to a particle phase, which is beneficial to deformation. However, the deformation behavior of the solution-treated $Mg_{94}Zn_{2.5}Y_{2.5}Mn_1$(at%) alloy has not been investigated until now. It is, therefore, necessary to study the relationship between deformation behavior and deformation parameters to obtain desired microstructure and mechanical properties.

In previous studies, the constitutive equation, dynamic recrystallization (DRX) kinetic model and processing map have been applied to understand the hot deformation behavior of magnesium alloys based on hot compression tests [22–30]. The Constitutive equation can be used to describe the relationship between flow stress and deformation conditions [3,5,6,17,22–26,28,30]. The DRX kinetic model has been used to provide information on the DRX fraction and predict the DRX evolution [22,23,26,27]. Processing map based on the dynamic material model (DMM) can be applied to control microstructures, optimize workability and avoid defects [4,6,22,24–26,28–30]. In this work, the flow stress curves of the solution-treated $Mg_{94}Zn_{2.5}Y_{2.5}Mn_1$ alloy under different deformation conditions were plotted, the DRX kinetic model and DMM processing maps were established using the hot compression experimental data, which can provide indispensable information for deformation parameters. Finally, a hot extrusion test was performed to verify the reasonability of the optimal deformation parameters.

2. Experimental procedures

The experimental $Mg_{94}Zn_{2.5}Y_{2.5}Mn_1$ (at%) alloy was prepared with high-purity Mg, Zn, Y, and Mn using an electric resistance furnace for melting under the protection of an atmosphere of Ar gas at 1023 K. Then, the alloy was cast into a preheated die at 993 K. The cast ingot with a diameter of 30 mm and a height of 150 mm was performed by solution treatment at 500 °C for 40 h. Cylindrical specimens with dimension of ϕ8mm × 12 mm were cut from the solution-treated ingot by aligning their axis along the length of cast ingot.

Isothermal axisymmetric hot compression tests of the solution-treated $Mg_{94}Zn_{2.5}Y_{2.5}Mn_1$ alloy were performed on a Gleeble-1500D thermal simulator testing machine at temperatures ranging from 350 °C to 500 °C, strain rates between 0.001 s^{-1} and 1 s^{-1} and a strain of 0.9. Each specimen was first heated to the deformation temperature at a heating rate of 10 °C/s and held at that temperature for 180 s to eliminate any thermal gradient before compression. After being compressed to the strain of 0.9, the specimen was immediately quenched in water and then sectioned parallel to the compression axis. Fig. 1 shows the schematic diagram of the hot compression tests. The initial microstructure and cutting samples were prepared by conventional methods for microstructural observations using optical microscopy (OM, Leica-DM2500 M), scanning electron microscopy (SEM, TESCAN-MIRA3) equipped with energy dispersive spectroscopy (EDS) and transmission electron microscopy (TEM, JEOL, 2010). The phase constitutions were analyzed by X-ray diffraction (XRD, Y-2000) with a Cu target.

3. Results and discussion

3.1. Initial microstructure

The Optical microstructures of as-cast and solution-treated

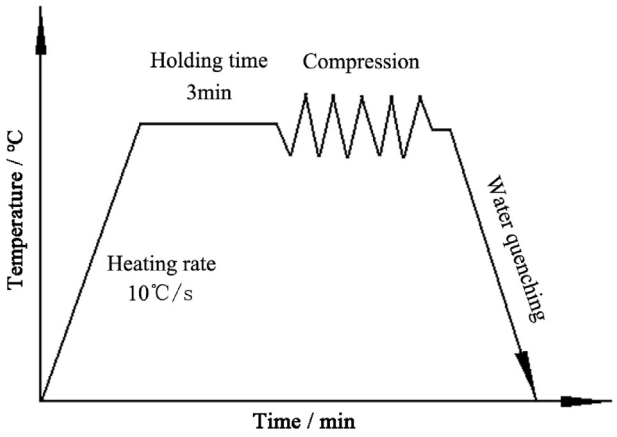

Fig. 1. Schematic diagram of hot compression tests.

$Mg_{94}Zn_{2.5}Y_{2.5}Mn_1$ alloys were shown in Fig. 2(a) and Fig. 2(b), respectively. The average grain size of α-Mg increased from 20.6 μm to 30.2 μm during solution treatment. Fig. 2(c) shows the SEM image of the as-cast $Mg_{94}Zn_{2.5}Y_{2.5}Mn_1$ alloy, indicating that the alloy consist of α-Mg matrix, block second phase and network second phase. After solution treatment, the partial block second phase along the grain boundaries transformed into the fine lamellar phase, which was homogeneously distributed in the grain interior. In addition, the network second phase transformed from a continuous network to a particle phase. The EDS results and XRD pattern reveal that the lamellar and particle phases are LPSO phase and W phase, respectively (Fig. 3). The TEM image and corresponding selected area electron diffraction (SAED) pattern show that the block second phase is 18R LPSO phase and the lamellar second phase is 14H LPSO phase。

The microstructure of the solution-treated $Mg_{94}Zn_{2.5}Y_{2.5}Mn_1$ alloy before the hot compression was confirmed to be composed of α-Mg, block 18R LPSO phase and particle W phase located at the grain boundaries, as well as lamellar 14H LPSO phase distributed in the grain interior.

3.2. Flow stress

The flow stress curves of the solution-treated $Mg_{94}Zn_{2.5}Y_{2.5}Mn_1$ alloy obtained at different temperatures and strain rates are presented in Fig. 4. It was found that all of flow stress curves exhibit the typical characteristics of DRX [26,31]. Certainly, there are also some differences that can be observed from the curves. At higher temperatures (450 °C, 500 °C), the variation of the flow stress can be divided into four stages due to the dynamic competition of the work hardening rate and the dynamic softening rate: the work hardening stage, the transition stage, the softening stage and the steady stage [26,27,32,33]. In the first stage, the flow stress increases sharply since the hardening rate resulting from dislocation generation and multiplication is higher than the softening rate caused by dynamic recovery (DRV). In the transition stage, although the softening effects of DRV are enhanced as the strain increases, the work hardening effects cannot be counteracted, leading to a continuous increase of the flow stress up to the peak stress and then DRX occurs. In the softening stage, the flow stress subsequently decreases after the peak stress with the further increase of true strain, which is due to the softening rate caused by DRX and DRV is higher than the hardening rate. Finally, the flow stress reaches the steady stage owing to the balance between the softening effects and the hardening effects. While the steady state cannot be observed at lower temperatures (350 °C, 400 °C), this